Research Square

Preprints are preliminary reports that have not undergone peer review.
They should not be considered conclusive, used to inform clinical practice,
or referenced by the media as validated information.

From Quantification to Differentiation: T2 Mapping for Mucinous Components in Primary and Post-neoadjuvant Rectal Cancers

Xiangpeng Xi
The First Affiliated Hospital of Shandong First Medical University & Shandong Provincial Qianfoshan Hospital

Qiang Zhao
The First Affiliated Hospital of Shandong First Medical University & Shandong Provincial Qianfoshan Hospital

Aiyin Li
The First Affiliated Hospital of Shandong First Medical University & Shandong Provincial Qianfoshan Hospital

Hongyu Zhao
The First Affiliated Hospital of Shandong First Medical University & Shandong Provincial Qianfoshan Hospital

Gesheng Song
songgesheng921@126.com

The First Affiliated Hospital of Shandong First Medical University & Shandong Provincial Qianfoshan Hospital

Research Article

Keywords: T2 mapping, rectal cancer, mucinous adenocarcinoma, neoadjuvant chemoradiotherapy, quantitative imaging, mucinous degeneration

Posted Date: September 7th, 2026

DOI: https://doi.org/10.21203/rs.3.rs-10793928/v1

License: This work is licensed under a Creative Commons Attribution 4.0 International License.
Read Full License

Additional Declarations: No competing interests reported.

From Quantification to Differentiation: T2 Mapping for Mucinous Components in Primary and Post-neoadjuvant Rectal Cancers

Abstract

Objective: To quantitatively assess mucin content in rectal mucinous adenocarcinoma and adenocarcinoma with mucinous components using T2 mapping, and to further evaluate its performance in distinguishing post-neoadjuvant chemoradiotherapy (nCRT) mucinous degeneration from primary rectal mucinous adenocarcinoma, thereby providing reliable imaging evidence for individualized treatment strategies.

Methods: This study consisted of two interrelated phases. Phase 1 investigated the correlation between T2 values and tumor mucin content. Phase 2 evaluated the diagnostic efficacy of T2 mapping for differentiating post-nCRT mucinous degeneration from primary mucinous adenocarcinoma. Patients who underwent rectal cancer surgery at our institution between January 2021 and June 2025 were retrospectively reviewed. For Phase 1, 55 patients were enrolled and divided into three groups based on postoperative pathological mucin content: mucinous adenocarcinoma group (MAC, mucin ≥50%, n=15); adenocarcinoma with mucinous component group (AMC, mucin <50%, n=20); and conventional adenocarcinoma group (AC, no mucin component, n=20). For Phase 2, 27 patients were enrolled, including 12 with post-nCRT mucinous degeneration and 15 with primary mucinous adenocarcinoma. All patients underwent pelvic MRI including T2 mapping within 1-2 weeks before surgery. Two radiologists independently performed ROI delineation. For Phase 1, ROIs were drawn along the tumor margin covering all tumor parenchyma while avoiding necrosis, cystic areas, and intraluminal contents. For Phase 2, ROIs were restricted to mucinous areas (hyperintense on T2-weighted images). Mean T2 values (ms) were automatically calculated. Phase 1 used univariate and multivariate regression to assess correlation with mucin content and diagnostic performance among the three groups. Phase 2 compared T2 values between the two groups and performed ROC curve analysis.

Results: (1) Phase 1: T2 values showed a strong positive correlation with pathological mucin content ($Rs = 0.877$, $P < 0.001$). Significant differences in T2 values were observed among the three groups ($P < 0.001$). For distinguishing AC from AMC, the AUC was 0.8175, sensitivity 0.95, specificity

0.70, optimal cutoff value 89.14 ms. Leave-one-out cross-validation (LOOCV) confirmed the robustness of this cutoff (mean 89.58 ms, range 89.14–90.01 ms), with a cross-validated AUC of 0.805. For distinguishing AMC from MAC, the AUC was 0.9867, sensitivity 0.93, specificity 1.00, optimal cutoff value 117.92 ms. LOOCV yielded a mean cutoff of 118.02 ms (range 117.41–121.97 ms) and a cross-validated AUC of 0.930. (2) Phase 2: T2 values in the post-nCRT mucinous degeneration group (median, 156.34 ms) were significantly lower than those in the primary MAC group (median, 198.76 ms; $P < 0.05$). The AUC for differentiating the two groups was 0.825, sensitivity 0.83, specificity 0.80, optimal cutoff value 181.92 ms. LOOCV demonstrated a mean cutoff of 187.91 ms (range 187.84–187.93 ms) and a cross-validated AUC of 0.772.

Conclusion: T2 mapping enables quantitative assessment of mucin content in rectal cancer, demonstrating a strong positive correlation with pathological mucin content and effective discrimination among MAC, AMC, and AC. Furthermore, T2 mapping effectively distinguishes post-nCRT mucinous degeneration from primary mucinous adenocarcinoma, providing a potential imaging tool for preoperative evaluation that may assist in treatment planning pending prospective validation.

Keywords: T2 mapping; rectal cancer; mucinous adenocarcinoma; neoadjuvant chemoradiotherapy; quantitative imaging; mucinous degeneration

Introduction

Rectal cancer remains one of the most common malignant tumors of the digestive tract worldwide, with persistently high incidence and mortality rates. Mucinous adenocarcinoma is a distinct histological subtype, accounting for approximately 10%–20% of all colorectal cancers [1-3]. According to the World Health Organization definition, mucinous adenocarcinoma is diagnosed when extracellular mucin accounts for ≥50% of the total tumor volume [4]. Compared with non-mucinous adenocarcinoma, mucinous adenocarcinoma exhibits distinct biological behaviors, including a stronger tendency for local invasion, higher rates of local recurrence, poorer response to neoadjuvant chemoradiotherapy (nCRT), and consequently an unfavorable prognosis [4, 5].

Mucin content itself has important clinical implications. Extracellular mucin forms a physical barrier that hinders the cytotoxic effects of chemotherapy and radiotherapy. Studies have shown that active mucin secretion is significantly associated with non-response or poor response to nCRT, and patients with high mucin expression have significantly shorter locoregional recurrence-free survival and distant metastasis-free survival [6]. Furthermore, mucinous differentiation (i.e., increased

extracellular mucin) is closely associated with immunosuppressive cell infiltration [7], which can attenuate anti-tumor immune responses and promote tumor progression. These findings, from molecular and histopathological perspectives, indicate that mucin-related features ultimately manifest as increased extracellular mucin content. Therefore, non-invasive and quantitative preoperative assessment of mucin content in rectal cancer could help predict response to nCRT, evaluate the risk of local recurrence, and guide individualized treatment strategies.

Neoadjuvant chemoradiotherapy has become the standard of care for locally advanced rectal cancer, aiming to achieve tumor downstaging, increase R0 resection rates, and reduce local recurrence [8]. After nCRT, some non-mucinous adenocarcinomas may develop treatment-induced mucinous degeneration [9], which indicates a good treatment response, whereas primary or residual mucinous adenocarcinoma generally has a poorer prognosis. However, both conditions present as hyperintense signals on conventional T2-weighted MRI, making them difficult to distinguish [10, 11]. This diagnostic dilemma may lead to unnecessary radical surgery or delayed curative treatment, highlighting the urgent need for reliable imaging methods to address this issue.

T2 mapping is a quantitative MRI technique that generates parametric maps reflecting tissue water content and macromolecular environment by acquiring multiple echoes and fitting T2 relaxation times. Previous studies have confirmed that T2 mapping has good diagnostic value in differentiating mucinous from non-mucinous rectal cancer [12]. However, that study only compared classic mucinous adenocarcinoma (mucin ≥50%) with non-mucinous adenocarcinoma and did not include intermediate-type tumors with mucin content between 1% and 49%. It has been shown that these adenocarcinomas with a mucinous component have intermediate immune microenvironment characteristics and prognosis between the two extremes [7, 13], but their quantitative T2 mapping features remain unclear. Moreover, whether T2 mapping can distinguish treatment-induced mucinous degeneration (acellular mucin) from primary or residual mucinous adenocarcinoma (cellular mucin) has not been systematically evaluated. Therefore, this study was divided into two parts to investigate the ability of T2 mapping to quantitatively assess mucin content in rectal cancer and its diagnostic performance in differentiating post-nCRT mucinous degeneration from primary mucinous adenocarcinoma.

Materials and Methods

Study Design and Patient Population

This retrospective case-control study was approved by the Institutional Review Board of our Hospital. The requirement for written informed consent was waived due to the retrospective nature of the study. The study was conducted in accordance with the Declaration of Helsinki.

The study comprised two independent but complementary phases, with patient cohorts derived from the same institutional database of patients who underwent surgery for rectal cancer between January 2021 and June 2025.

Phase 1: Correlation between T2 Values and Mucin Content

Inclusion criteria: (1) pathologically confirmed rectal adenocarcinoma (including mucinous adenocarcinoma, adenocarcinoma with mucinous component, and conventional adenocarcinoma); (2) preoperative pelvic MRI including T2 mapping performed within 1–2 weeks before surgery; (3) complete histopathological data available.

Exclusion criteria: (1) prior pelvic radiotherapy or chemotherapy; (2) poor image quality precluding accurate ROI delineation; (3) other synchronous malignancies.

Phase 2: Differentiation between Post-nCRT Mucinous Degeneration and Primary Mucinous Adenocarcinoma

Inclusion criteria: (1) pathologically confirmed diagnosis of either primary rectal mucinous adenocarcinoma or significant mucinous degeneration after nCRT; (2) preoperative pelvic MRI including T2 mapping; (3) complete clinical and pathological data.

Exclusion criteria: (1) poor image quality; (2) incomplete pathological assessment.

Sample Size Estimation

For Phase 2, an a priori sample size estimation was performed using G*Power software. Assuming equal group allocation, we used a two-sample mean comparison model with a moderate-to-large effect size (Cohen's $d = 0.8$), two-tailed $\alpha = 0.05$, and power = 0.80. The calculation indicated that at least 13 patients per group were needed, with a total sample size of no less than 26. The actual sample size in this study was 27 (12 in the post-nCRT group and 15 in the primary MAC group). Although the group sizes were not perfectly equal, the total sample size met the estimation requirement, and the statistical power recalculated based on the actual allocation ratio remained close to 0.80, confirming sufficient power to detect significant differences in T2 values between the two groups.

MRI Acquisition

All patients underwent MRI within 1–2 weeks before surgical resection, an interval consistent with routine clinical practice and considered acceptable for imaging-pathology correlation studies [14]. For patients receiving neoadjuvant chemoradiotherapy (nCRT), MRI was performed at a standardized restaging interval of 6–8 weeks after completion of nCRT [15-17], followed by surgery within the subsequent 1–2 weeks. No intervening treatment was administered during this period,

and previous studies have confirmed that treatment-induced fibrosis and mucinous degeneration reach a relatively stable plateau at the time of restaging [18]; therefore, significant changes in T2 values or mucin content during this interval are unlikely.

All patients underwent pelvic MRI on a 3.0T scanner (Discovery 750; GE Healthcare) using an 8-channel phased-array surface coil. Standardized bowel preparation was performed 30 minutes before the examination, including: (1) cleansing enema; (2) intramuscular injection of 10 mg anisodamine to reduce intestinal peristalsis; and (3) instillation of approximately 60–100 mL of ultrasonic coupling gel (mixed with water at a 1:1 ratio) into the rectum for moderate distension.

The T2 mapping sequence was acquired using a multi-echo spin-echo sequence with the following parameters: TR 1062 ms; TE 12.1–95.7 ms (8 echoes); slice thickness 3 mm; interslice gap 0 mm; FOV 18 × 18 cm; matrix 224 × 160; acquisition time 6 min 36 s. Additional conventional sequences (sagittal T2WI, oblique axial HR-T2WI, and coronal T2WI) were also obtained for clinical staging but were not used for quantitative analysis in this study. Detailed sequence parameters are shown in Table 1.

Table 1. MRI Sequence Parameters

Sequence	TE (ms)	TR (ms)	FOV (cm)	Slice thickness (mm)	Interslice gap (mm)	Matrix	Acquisition time (s)
Sagittal T2WI	85	8137	27	4	0.4	352×352	199
Oblique axial HR-T2WI	102	5868	18	3	0	320×288	286
Coronal T2WI	90	7382	32	4	0.4	480×480	231
T2 mapping	12.1-95.7	1062	18	3	0	224×160	396

Note: TE, echo time; TR, repetition time; FOV, field of view; HR, high resolution.

Image Analysis

All images were transferred to an Advantage Workstation (version AW 4.6; GE Medical System). Prototype software (Function tool MADC; GE Healthcare) was used to process the T2 mapping sequence and generate parametric maps. Two radiologists with experience in abdominal imaging, who were blinded to the patients' clinical and pathological information, independently performed image processing. For each slice containing the tumor, regions of interest (ROIs) were delineated with reference to the oblique axial high-resolution T2-weighted images. In Phase 1, ROIs were manually drawn along the tumor margin slice by slice, attempting to include all solid components of the tumor while avoiding macroscopically visible necrosis, cystic areas, and intraluminal contents. In Phase 2, ROIs were delineated only over the mucinous areas within the tumor (which appeared

hyperintense on the corresponding T2-weighted images). The post-processing software automatically calculated the corresponding T2 values (in ms) based on the multi-slice ROIs, and the mean T2 value of all slices was taken as the final T2 value for each tumor for statistical analysis.

Interobserver agreement for ROI delineation was assessed using intraclass correlation coefficients (ICC) based on a randomly selected subset of 10 patients from each phase, analyzed by the two independent radiologists. If the interobserver agreement was low, a senior radiologist re-evaluated the ROIs. A unified MRI protocol, T2 mapping post-processing workflow, and ROI measurement criteria were applied consistently across both phases to ensure data comparability.

After acquiring images at multiple echo times, the signal intensity as a function of TE for each pixel was fitted to calculate the T2 value. The most commonly used fitting model is the mono-exponential decay model:

$$S(TE) = S_o \cdot e\text{^}(-TE/T2)$$

where S(TE) is the signal intensity at time TE, and S_0 is the initial signal intensity (at TE = 0). The T2 value for each pixel was obtained by nonlinear least-squares fitting. The T2 values of all pixels were displayed as a pseudo-color map, which constitutes the T2 map.

Tumor Assessment and Image Information Acquisition

Two radiologists performed preoperative structured reporting for rectal cancer patients according to the Chinese Society of Clinical Oncology (CSCO) colorectal cancer diagnosis and treatment guidelines [19], recording the mrTN stage and mrEMVI status. mrEMVI positivity was defined as a Smith score ≥ 3 (5-point scale: 0 = definitely absent; 1 = probably absent; 2 = uncertain; 3 = probably present; 4 = definitely present). T-stage criteria were as follows: T1 = invasion of the submucosa; T2 = invasion of the muscularis propria; T3 = penetration through the muscularis propria into the subserosa/mesorectum/intersphincteric space; T4 = invasion of the visceral peritoneum or adjacent organs. Positive lymph node metastasis was defined as a short-axis diameter ≥ 8 mm, or a short-axis diameter > 5 mm together with at least one of the following features: heterogeneous signal, irregular shape, or ill-defined margin. Any disagreements between the two radiologists were adjudicated by a senior radiologist with 20 years of experience in rectal cancer diagnosis.

Fasting peripheral venous blood was collected within one week before surgery, and serum was separated by centrifugation within 2 hours after collection. Serum levels of carcinoembryonic antigen (CEA) and carbohydrate antigen 19-9 (CA19-9) were measured using

electrochemiluminescence immunoassay (ECLIA). The normal reference ranges were 0–5 ng/mL for CEA and 0–37 U/mL for CA19-9; values above the upper limit of normal were defined as positive.

Pathological Features

Pathological diagnosis and mucin content assessment were independently performed by two deputy chief pathologists. Postoperative specimens were fixed in formalin, sampled according to standardized protocols, with emphasis on the deepest area of tumor invasion and areas showing obvious mucin signal on MRI. All specimens were embedded in paraffin, serially sectioned (4 μm), and stained with hematoxylin and eosin (HE). Histological classification was performed according to the 5th edition of the WHO classification of digestive system tumors [20]: mucinous adenocarcinoma (MAC) was defined as extracellular mucin accounting for ≥50% of the tumor volume, with tumor cells floating in mucin lakes; adenocarcinoma with mucinous component (AMC) was defined as the presence of definite mucin but <50%; adenocarcinoma (AC) was defined as no mucin or <5% (according to routine pathological reporting criteria). Mucin content was assessed using the area percentage method: representative sections were selected at low magnification (40× or 100×), and the percentage of mucin area relative to the tumor parenchyma (tumor cells and stroma, excluding normal bowel wall, necrosis, and inflammatory exudate) was estimated. When mucin distribution was uneven, the mean value from multiple fields and multiple tissue blocks was taken.

For patients who underwent surgery after neoadjuvant chemoradiotherapy, the specimens were evaluated according to the College of American Pathologists (CAP) tumor regression grading system [21]. The key distinction was made between cellular mucin (visible viable tumor cells within or adjacent to mucin lakes, indicating incomplete treatment response) and acellular mucin (no viable tumor cells within or adjacent to mucin lakes, only mucinous material, which may be accompanied by histiocytic infiltration, foam cell accumulation, and fibrosis, indicating pathological complete response). Adequate sampling and comprehensive observation were required; when necessary, serial sections or immunohistochemistry (e.g., CK20, CK7) were performed to aid in identifying scattered residual tumor cells.

Imaging-pathology correlation

Pathological specimens were reviewed and photographed after formalin fixation. MRI slices were qualitatively matched to gross pathological sections and corresponding hematoxylin-and-eosin (HE)-stained slides using anatomical landmarks, including tumor location relative to the anal verge, tumor morphology, and adjacent mesorectal structures. The MRI slice that best corresponded to each pathological section was identified by consensus between two radiologists and two pathologists. For Phase 1, the whole-tumor ROI on MRI was correlated with the overall mucin

percentage estimated from the corresponding pathological block. For Phase 2, ROIs were placed on mucinous areas (hyperintense on T2WI) and qualitatively matched to mucin lakes identified on histology. Due to the retrospective design, formal co-registration using fiducial markers or specimen orientation was not performed; instead, matching was performed at the whole-tumor or regional level.

Statistical Analysis

Statistical analyses were performed using SPSS 26.0 (IBM, Armonk, NY, USA), MedCalc 20.0 (MedCalc, Mariakerke, Belgium), and R software (version 4.3, R Foundation for Statistical Computing, Vienna, Austria). Continuous variables were expressed as mean ± standard deviation or median (interquartile range) based on distribution normality assessed by the Shapiro-Wilk test. Categorical variables were presented as frequencies and percentages.

Phase 1 Analysis: Spearman's rank correlation coefficient (Rs) was used to assess the correlation between T2 values and pathological mucin content. Differences in T2 values among the three groups (AC, AMC, and MAC) were evaluated using the Kruskal-Wallis test, followed by post-hoc pairwise comparisons (Mann-Whitney U test with Bonferroni correction). Receiver operating characteristic (ROC) curve analysis was performed to evaluate the diagnostic performance of T2 values for distinguishing AC from AMC and AMC from MAC, with calculation of the area under the curve (AUC), the optimal cutoff value determined by the Youden index, sensitivity, and specificity. Univariate and multivariate logistic regression analyses were conducted to identify clinical characteristics (age, sex, carcinoembryonic antigen level, T stage, N stage, and extramural vascular invasion) potentially influencing mucin content.

Phase 2 Analysis: The Mann-Whitney U test was used to compare T2 values between the post-nCRT mucinous degeneration group and the primary mucinous adenocarcinoma group. ROC curve analysis was performed to evaluate the diagnostic performance of T2 values for distinguishing the two groups, with calculation of the AUC, optimal cutoff value, sensitivity, and specificity.

Internal Validation: To internally validate the robustness of the optimal T2 cutoffs derived from the original cohorts, leave-one-out cross-validation (LOOCV) was performed separately for each diagnostic comparison (AC vs. AMC, AMC vs. MAC, and Phase 2). In each LOOCV iteration, one patient was excluded as the test set, and the remaining patients served as the training set. The Youden index-based optimal cutoff was re-determined on each training set and applied to classify the excluded patient. The distribution of the optimal cutoffs across all iterations (mean and range) was calculated to assess threshold stability. The cross-validated predictive performance was evaluated using two approaches: (1) the area under the ROC curve (AUC) based on the original T2 values,

which remains identical to the discovery cohort due to the rank-invariant nature of the AUC metric, and (2) the AUC based on logistic regression-derived probabilities from each training set (Logit-LOOCV AUC), which reflects the true generalizable predictive performance. Accuracy, sensitivity, and specificity were also calculated from the aggregated cross-validated classifications. All LOOCV procedures were implemented using R software with the pROC package.

To assess interobserver reproducibility, ROI delineation was independently performed by two radiologists on a randomly selected subset of 10 patients from each phase. Interobserver agreement was evaluated using the intraclass correlation coefficient (ICC) based on a two-way random-effects model for absolute agreement [ICC(2,1)]. ICC values were interpreted as: <0.5, poor; 0.5–0.75, moderate; 0.75–0.9, good; >0.9, excellent. The 95% confidence intervals (CIs) for ICC were calculated using bootstrap resampling (1000 iterations).

Results

Patient Characteristics

Phase 1 Cohort: A total of 55 patients were included in Phase 1 of this study. Based on postoperative pathological mucin content, patients were divided into three groups: mucinous adenocarcinoma (MAC) group, defined as mucin content ≥50% (n=15); adenocarcinoma with mucinous component (AMC) group, defined as mucin content <50% (n=20); and adenocarcinoma (AC) group, defined as no mucinous component (n=20). The distribution of mucin content (%) across the different pathological groups is shown in Table 2.

Table 2 Distribution characteristics of mucin content (%) in different pathological groups

Statistic	AMC (Mucin < 50%, n=20)	MAC (Mucin ≥ 50%, n=15)	Total (n=35)
Mean	24.25%	71.67%	44.57%
Deviation (SD)	13.56%	15.99%	27.39%
Median	20%	75%	40%
Minimum (Min)	5%	50%	5%
Maximum (Max)	45%	90%	90%
First Quartile (Q1)	10%	55%	20%
Third Quartile (Q3)	40%	85%	65%
Interquartile Range (IQR)	30%	30%	45%

It should be noted that mucinous adenocarcinoma accounts for a relatively low proportion of rectal cancers (approximately 4.6%–10%). During the study inclusion period (January 2021 to June 2025), a total of 15 patients with mucinous adenocarcinoma met the inclusion and exclusion criteria, and

all were enrolled. The 20 patients in the AMC group were consecutive cases with a clearly documented mucin content percentage (1%–49%) in the pathological reports. Adenocarcinoma (AC) is the most common type in clinical practice; however, to reduce confounding bias and achieve good matching with the sample size of the AMC group (thereby enhancing the balance of statistical comparisons among the three groups), 20 patients with pure adenocarcinoma (without any mucinous component) from the same period were selected using a random sampling method.

No statistically significant differences were observed among the three groups in terms of sex, mrTN stage, or mrEMVI (P > 0.05). Statistically significant differences were found among the three groups in age, CEA level, and CA19-9 level (P < 0.05). However, after Bonferroni correction for post-hoc pairwise comparisons, none of the pairwise differences in age reached statistical significance (P > 0.05) (Table 3).

Table 3 Clinical and radiological characteristics of patients in Phase 1

Characteristic	AC	AMC	MAC	P
Age (years)	58.65±13.73	67.85±12.03	67.27±9.65	0.038*
Sex, No. (%)				0.481
Male	13（65）	13（65）	7（47）	
Female	7（35）	7（35）	8（53）	
CEA(ng/mL)，No. (%)				0.046*
< 5	16（80）	9（45）	8（53）	
≥5	4（20）	11（55）	7（47）	
CA199(U/mL)，No. (%)				0.005*
< 37	18（90）	15（75）	12（80）	
≥37	2（10）	5（25）	3（20）	
mrT stage，No. (%)				0.665
T1-2	7（35）	6（30）	5（33.3）	
T3-4	13（65）	14（70）	10（66.7）	
mrT stage，No. (%)				0.440
mrN0	11（55）	10（50）	5（33.3）	
mrN1-2	9（45）	10（50）	10（66.7）	
mrEMVI，No. (%)				0.681
Positive	5（25）	4（20）	5（33.3）	
Negative	15（75）	16（80）	10（66.7）	

Note: CEA, carcinoembryonic antigen; CA19-9, carbohydrate antigen 19-9; mrT stage, magnetic resonance T stage; mrN stage, magnetic resonance N stage; mrEMVI, magnetic resonance extramural vascular invasion. $P < 0.05$ was considered statistically significant.

Phase 2 Cohort: According to the above criteria, a total of 27 patients were enrolled in this study, including 15 patients with primary rectal mucinous adenocarcinoma and 12 patients with significant mucinous degeneration after neoadjuvant chemoradiotherapy (nCRT). All patients in the post-nCRT group had completed standard long-course chemoradiotherapy (45–50.4 Gy in 25–28 fractions with concurrent capecitabine or 5-fluorouracil) and underwent surgery 6–8 weeks after completion of treatment. Pathologically, post-nCRT mucinous degeneration was defined as the presence of identifiable acellular mucin lakes within the tumor bed (regardless of area percentage), with residual viable tumor cells comprising less than 10% of the tumor bed area (i.e., major pathological response). Cases with no identifiable mucinous component or with residual tumor cells ≥10% were excluded. Among the 27 patients, 15 were male and 12 were female. No statistically significant differences were observed between the two groups in age, sex, CEA, CA19-9, mrTN stage, or mrEMVI ($P > 0.05$) (Table 4). In the post-nCRT group, pathological assessment confirmed that all 12 patients achieved major pathological response (tumor regression grade 1–2), with residual tumor cells <10% in all cases.

Table 4 Clinical and radiological characteristics of patients in Phase 2

Characteristic	Primary MAC Group	Mucinous Degeneration Group	P value
Age (years)	64.60±9.78	69.67±14.22	0.284
Sex, No. (%)			0.620
Male	9（66.7）	6（40）	
Female	6（33.3）	6（50）	
CEA(ng/mL)，No. (%)			0.741
< 5	7（46.7）	9（75）	
≥5	8（53.3）	3（25）	
CA199(U/mL)，No. (%)			0.086
< 37	8（53.3）	10（83.3）	
≥37	7（46.7）	2（16.7）	
mrT stage，No. (%)			0.925
T1-2	4（26.7）	5（41.7）	
T3-4	11（73.3）	7（58.3）	
mrT stage，No. (%)			0.431
mrN0	4（26.7）	3（25）	
mrN1-2	11（73.3）	9（75）	
mrEMVI，No. (%)			0.345
Positive	5（33.3）	2（16.7）	
Negative	10（66.7）	10（83.3）	

Interobserver Agreement

Interobserver agreement for T2 value measurements was excellent in both phases. The ICC was 0.997 (95% CI: 0.994–0.999) for Phase 1 and 0.952 (95% CI: 0.891–0.983) for Phase 2, indicating high reproducibility of ROI delineation across readers.

Phase 1: Quantitative Assessment of Mucin Content and Diagnostic Performance of T2 Mapping

T2 values showed a strong positive correlation with pathological mucin content (Rs = 0.877, P < 0.001; Figure 1). T2 values demonstrated a progressive increase across the three groups: AC group (mean 82.48 ± 5.35 ms), AMC group (92.86 ± 10.14 ms), and MAC group (160.73 ± 33.19 ms).

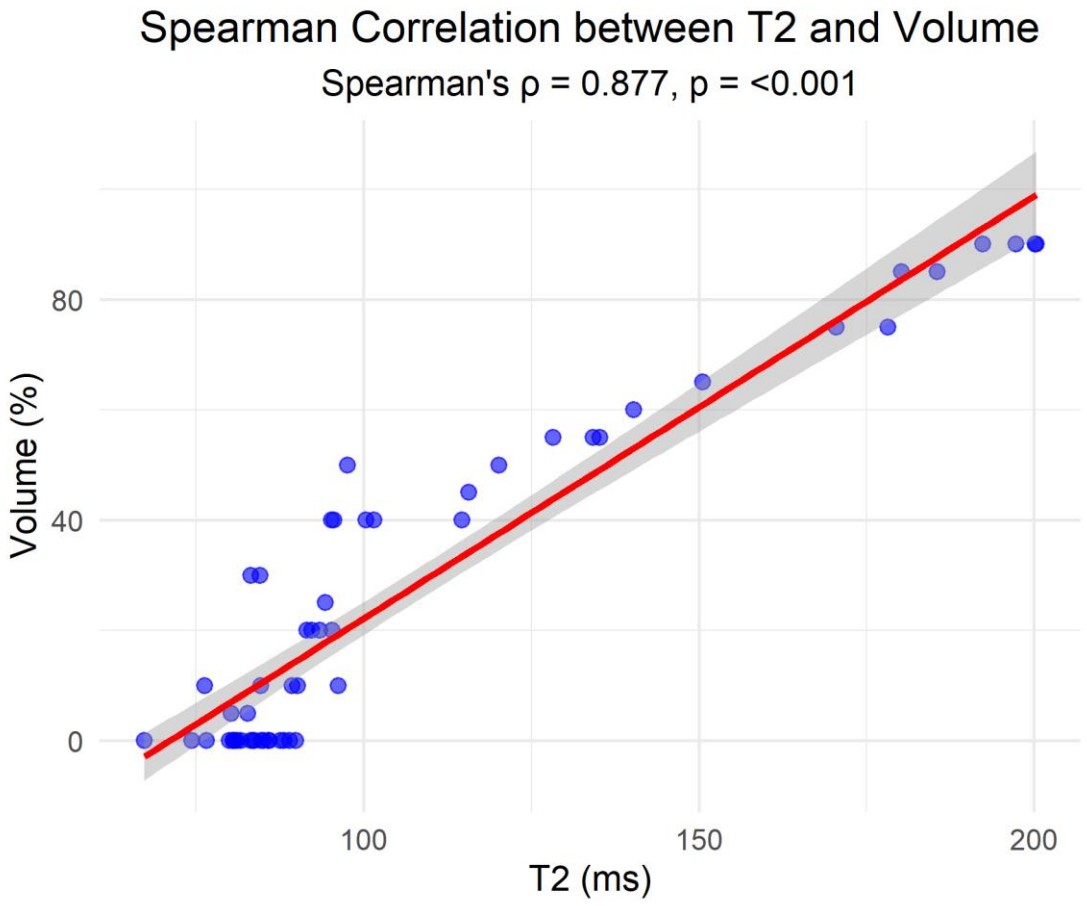


Figure 1. Correlation analysis between percentage of mucin content and T2 values. Spearman's rank correlation test revealed a significant positive correlation (Spearman r = 0.877, P = 1.51×10^{-18}). Blue scatter points represent individual sample data points. The solid blue line indicates the linear regression line, the light blue shaded area represents the 95% confidence interval, and the red dashed line represents the smoothed fitted trend line.

Significant differences in T2 values were observed among the three groups (Kruskal-Wallis test, $P < 0.001$; see Table 5). Post-hoc pairwise comparisons revealed significant differences between AC and AMC ($P < 0.001$), AC and MAC ($P < 0.001$), and AMC and MAC ($P < 0.001$).

Table 5 Comparison of T2 values among the three groups

Group	Number of cases	T2 value mean (ms)	P value
MAC	15	160.73±33.19	
AMC	20	92.86±10.14	P<0.001*
AC	20	82.48±5.35	

ROC curve analysis results are summarized in Table 6. T2 values demonstrated good to excellent diagnostic performance in distinguishing among the three pathological types of rectal adenocarcinoma (AC, AMC, and MAC). Notably, the T2 value ranges for AC and MAC were completely separated (AC: 67.251–89.868 ms; MAC: 97.566–200.350 ms), yielding an AUC of 1.000. Any cutoff value between 89.868 and 97.566 ms achieved 100% sensitivity and specificity. The optimal cutoff value determined by Youden's index was 93.717, corresponding to a sensitivity of 100% (15/15) and a specificity of 100% (20/20), with a Youden's index of 1.000. Using the bootstrap method with 100 resampling iterations to calculate the optimal cutoff value, a total of 14 unique values were obtained, with a median of 93.717, which was consistent with the result from the original sample. For distinguishing AC from AMC, the AUC was 0.8175 (95% CI: 0.691–0.943), with an optimal cutoff value of 89.14 ms, a sensitivity of 95.0%, and a specificity of 70.0% (Figure 2). For distinguishing AMC from MAC, the AUC was 0.9867 (95% CI: 0.966–1.000), with an optimal cutoff value of 117.92 ms, a sensitivity of 93.0%, and a specificity of 100% (Figure 3). For distinguishing MAC from non-MAC (i.e., AMC + AC), the AUC was 0.993 (95% CI: 0.979–1.000), with an optimal cutoff value of approximately 117.92 ms, a sensitivity of 93.3%, and a specificity of 100%. In addition, for distinguishing mucinous lesions (MAC + AMC) from AC, the AUC was 0.896 (95% CI: 0.810–0.981), with an optimal cutoff value of 90.01 ms, a sensitivity of 80.0%, and a specificity of 100%. These results indicate that T2 values have significant clinical value in distinguishing the subtypes of rectal adenocarcinoma, particularly in identifying pure mucinous adenocarcinoma.

Table 6. ROC analysis of optimal cut-off values and diagnostic performance of T2 values between different pathological groups

Comparison Group	AUC (95% CI)	Optimal cut-off (ms)	Se	Sp
AC vs. ACM	0.817 (0.691–0.943)	89.14	0.95	0.70
ACM vs. MAC	0.987 (0.966–1.000)	117.92	0.93	1.00
AC vs. MAC	1.000	89.868–97.566	1.00	1.00
MAC vs. non-MAC	0.993（0.979- 1）	117.915	0.93	1.00
MAC +AMC vs. AC	0.896 (0.810–0.981)	90.013	0.80	1.00

Note: Se = Sensitivity, Sp = Specificity

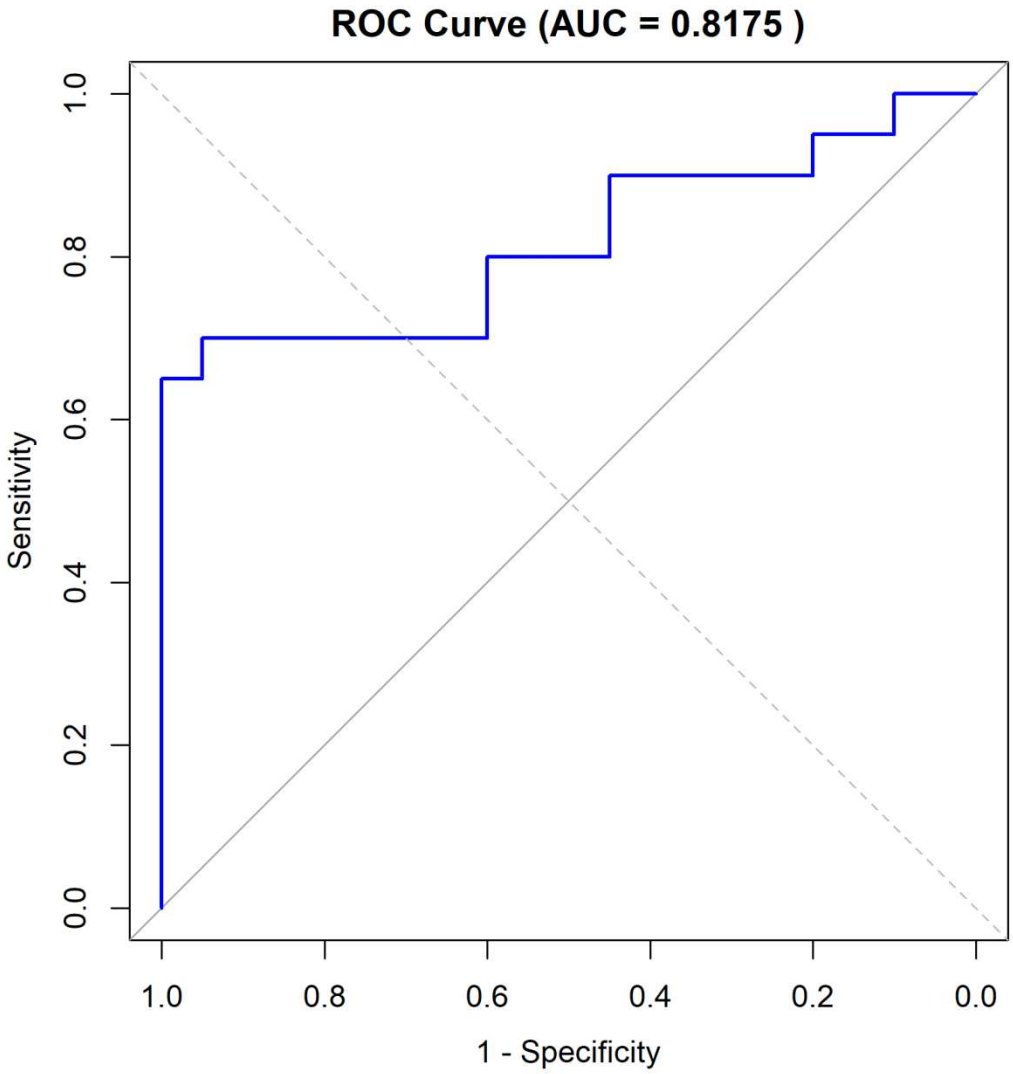


Figure 2. ROC curve analysis of T2 values for differentiating AC from AMC. The AUC was 0.8175 (95% CI: 0.691–0.943, $P < 0.001$).

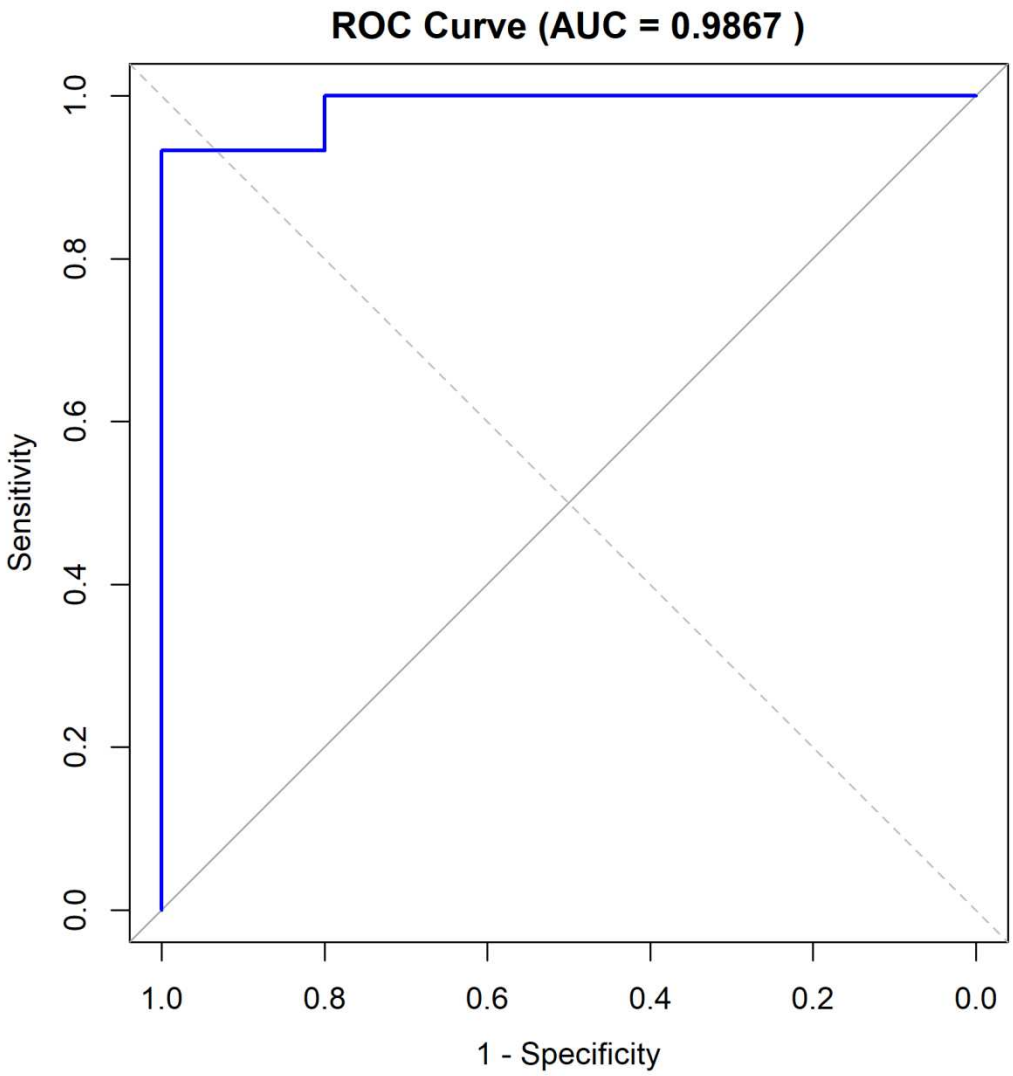


Figure 3. ROC curve analysis of T2 values for differentiating AMC from MAC. The AUC was 0.9867 (95% CI: 0.966–1.000, P < 0.001).

Multivariate regression analysis revealed that T2 value was the only independent predictor of mucin content after adjusting for age, sex, CEA level, and tumor stage (odds ratio per 1 ms increase: 1.12, 95% CI: 1.08–1.17, P < 0.001). Representative imaging and pathological findings of rectal cancers with varying mucin content are shown in Figures 4–6.

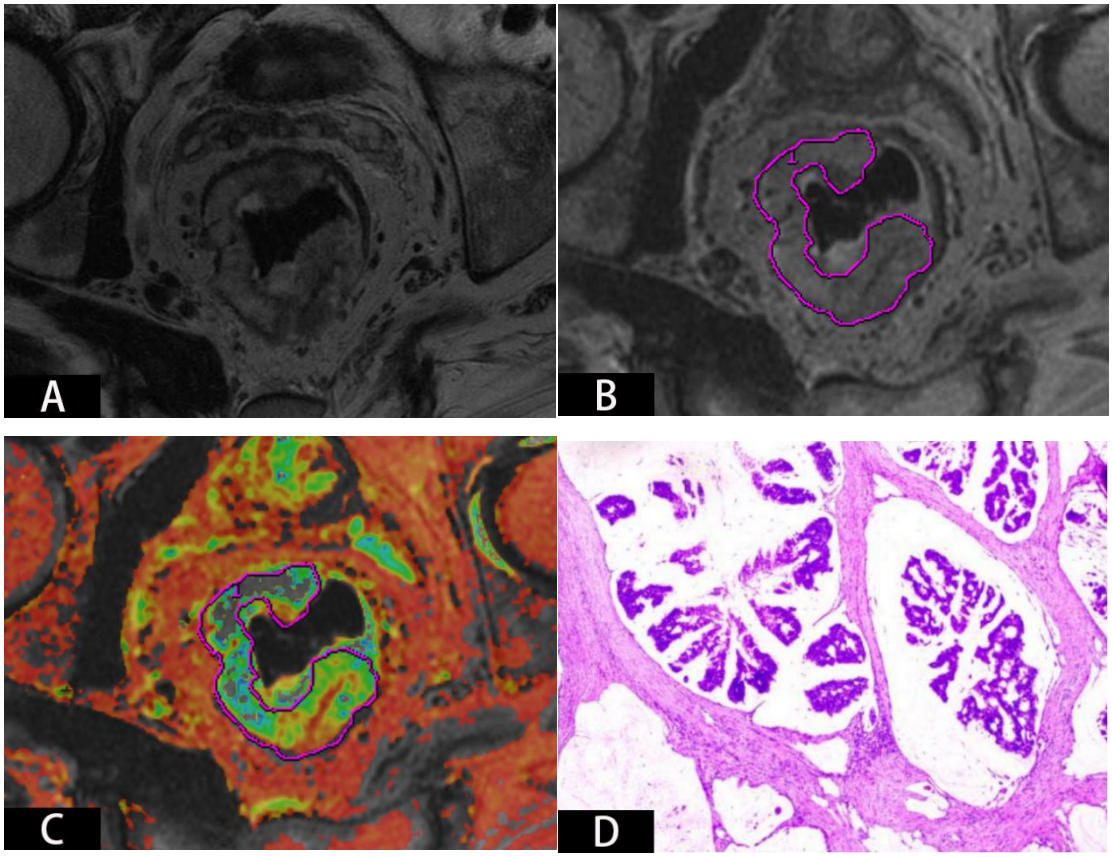
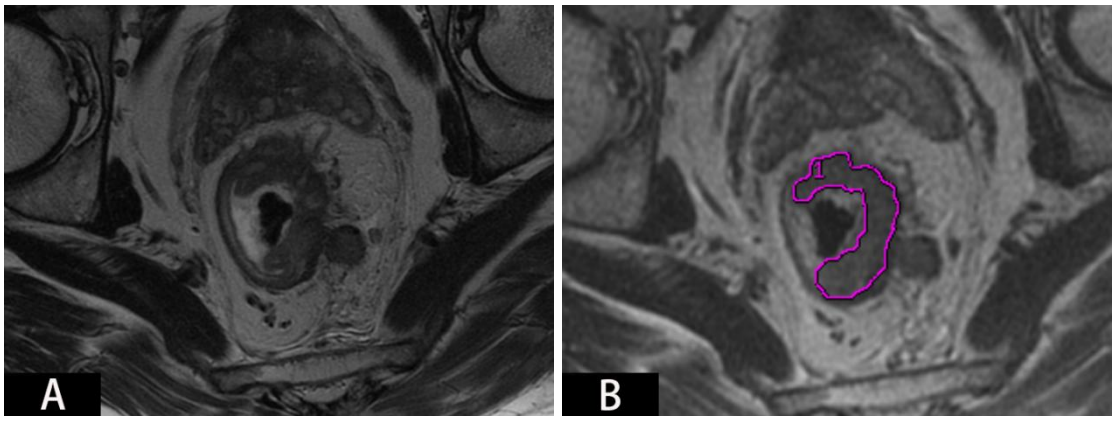


Figure 4. MRI and pathological images of rectal mucinous adenocarcinoma. A 64-year-old male patient with rectal mucinous adenocarcinoma and a mucin content of 75%. Figure 4A shows oblique axial T2-weighted image (T2WI); Figure 4B shows T2 mapping; Figure 4C shows the pseudo-color T2 map generated by post-processing; Figure 4D shows the pathological image (HE staining, high magnification). The T2 value was 178.23 ms.



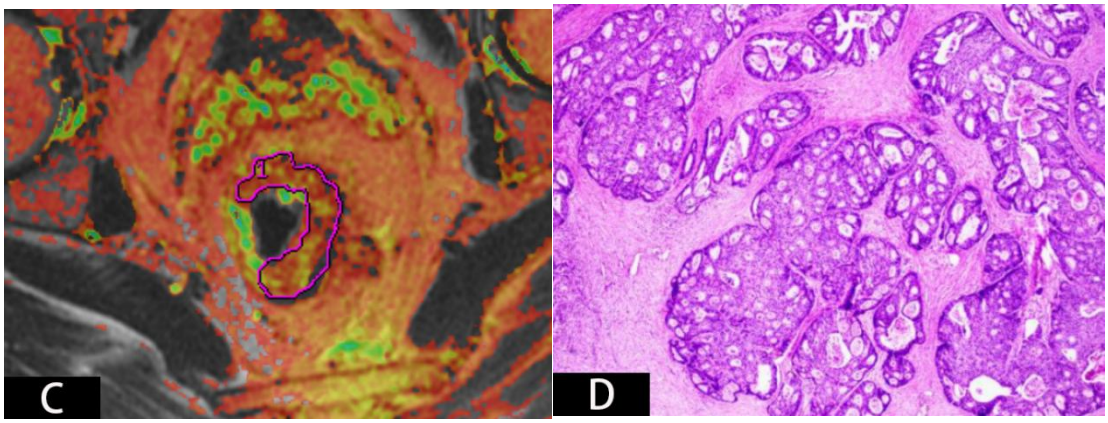


Figure 5. MRI and pathological images of rectal adenocarcinoma with mucinous component. A 71-year-old male patient with rectal adenocarcinoma with mucinous component and a mucin content of 10%. Figure 5A shows oblique axial T2-weighted image (T2WI); Figure 5B shows T2 mapping; Figure 5C shows the pseudo-color T2 map generated by post-processing; Figure 5D shows the pathological image (HE staining, high magnification). The T2 value was 90.159 ms.

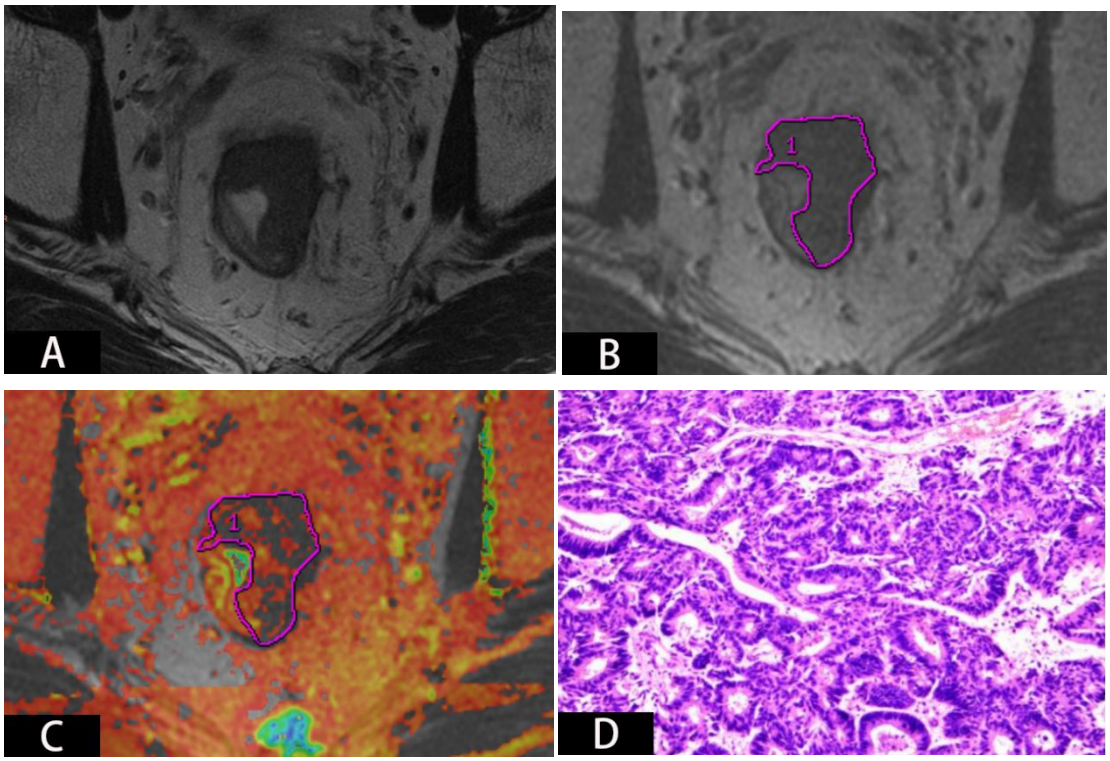


Figure 6. MRI and pathological images of rectal adenocarcinoma. A 59-year-old male patient with rectal adenocarcinoma. Figure 6A shows oblique axial T2-weighted image (T2WI); Figure 6B shows T2 mapping; Figure 6C shows the pseudo-color T2 map generated by post-processing; Figure 6D shows the pathological image (HE staining, high magnification). The T2 value was 85.809 ms.

Phase 2: Differentiation between Post-nCRT Mucinous Degeneration and Primary Mucinous Adenocarcinoma

T2 values differed significantly between the post-nCRT mucinous degeneration group and the primary mucinous adenocarcinoma group (P = 0.012). The median T2 value in the post-nCRT group was 198.76 ms (interquartile range: 182.34–214.23 ms), whereas that in the primary mucinous adenocarcinoma group was 156.34 ms (interquartile range: 142.21–168.45 ms) (see Table 7).

Table 7. Comparison of T2 values between the two groups

Group	Number of cases	T2 value mean (ms)	P value
Mucinous Degeneration Group	12	192.98±7.96	P=0.02*
MAC group	15	181.55±9.35	

ROC curve analysis demonstrated good diagnostic performance of T2 values for distinguishing the two groups (Figure 7). The AUC was 0.825 (95% CI: 0.672–0.978). Using the optimal cutoff value of 181.92 ms derived from the Youden index, the sensitivity was 0.83 and the specificity was 0.80 for distinguishing post-nCRT mucinous degeneration from primary mucinous adenocarcinoma. Representative cases and comparisons are shown in Figure 8.

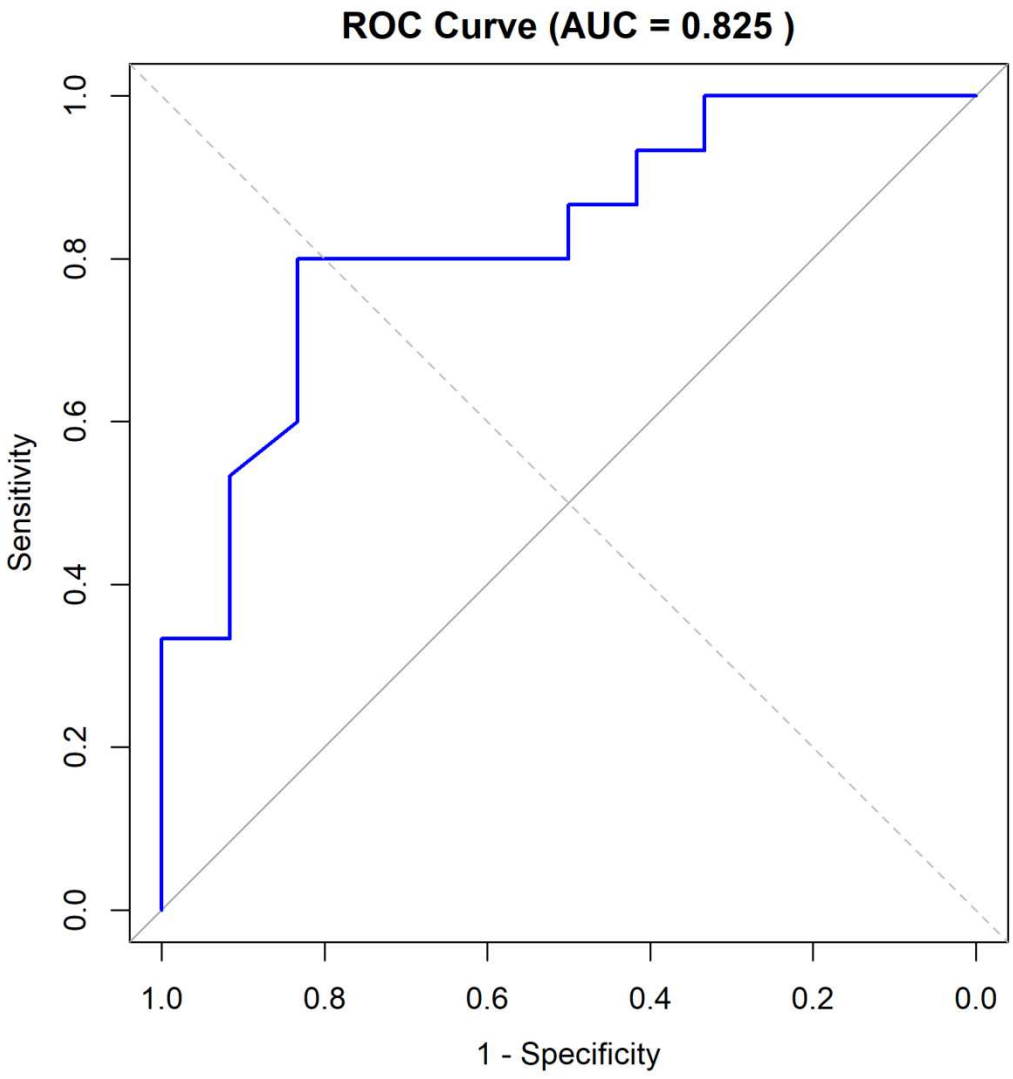
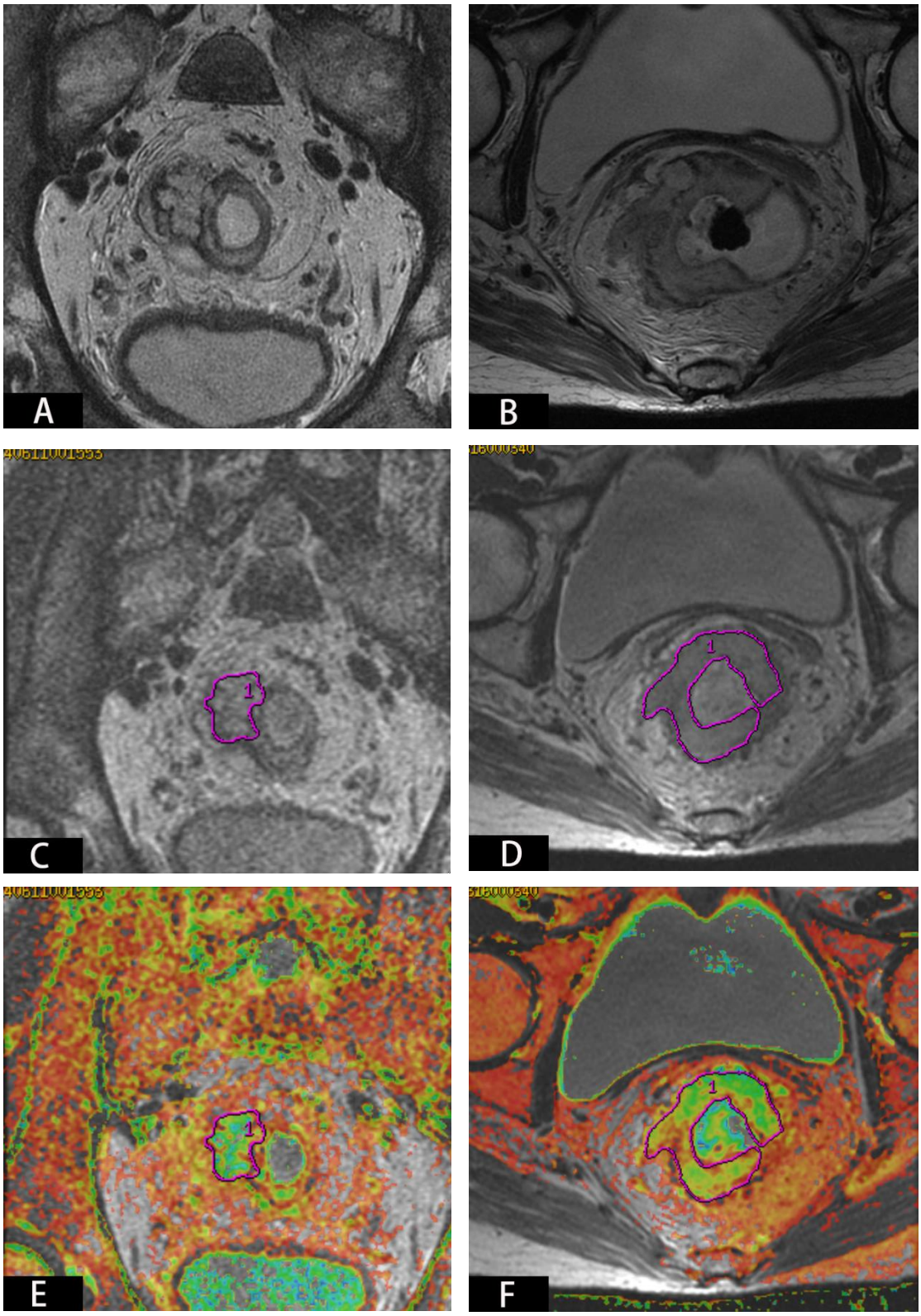


Figure 7. ROC curve for differentiating the mucinous degeneration group from the mucinous

adenocarcinoma group. The ROC curve was used to evaluate the performance of T2 values in distinguishing between the mucinous degeneration group and the mucinous adenocarcinoma group. The area under the curve (AUC) was 0.825 (95% CI: 0.631–0.943).



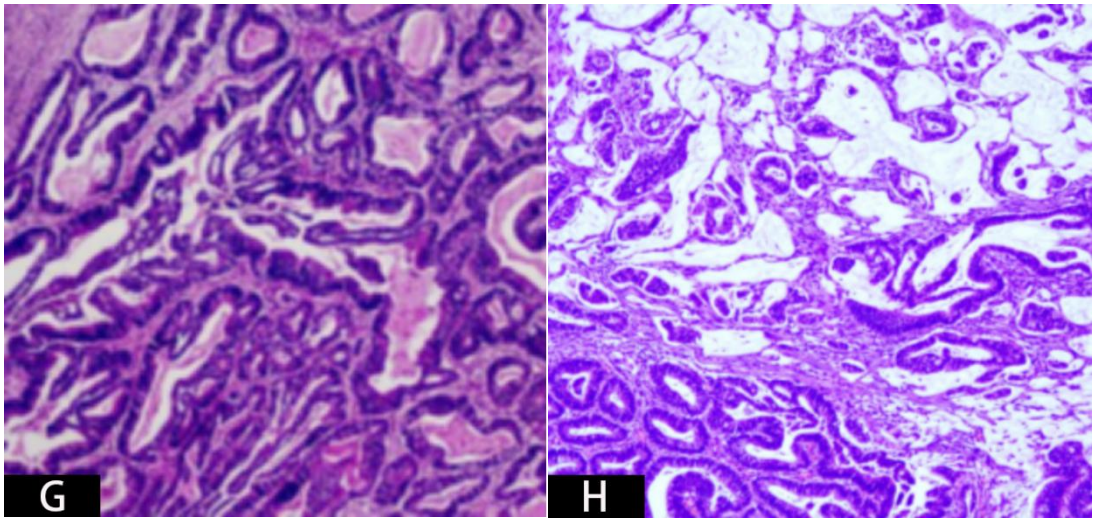


Figure 8. MRI and pathological images of mucinous degeneration after nCRT and mucinous adenocarcinoma of the rectum. Images A, C, E, G are from a patient with mucinous degeneration after nCRT. Figure 8A: oblique axial T2WI; Figure 8C: T2 mapping; Figure 8E: pseudo-color T2 map generated by post-processing; Figure 8G: pathological image (HE staining, high magnification). The T2 value was 203.157 ms. Images B, D, F, H are from a patient with mucinous adenocarcinoma. Figure 8B: oblique axial T2WI; Figure 8D: T2 mapping; Figure 8F: pseudo-color T2 map generated by post-processing; Figure 8H: pathological image (HE staining, high magnification). The T2 value was 180.765 ms. In Figure 8G, the pathological image shows acellular pure mucinous components, whereas in Figure 8H, tumor cells can be seen within the mucinous components.

Internal Validation of T2 Cutoffs

To assess the robustness of the optimal T2 cutoffs derived from the original cohorts, we performed leave-one-out cross-validation (LOOCV) separately for each diagnostic comparison (AC vs. AMC, AMC vs. MAC, and Phase 2). The results are summarized in Table 8.

Table 8. Leave-one-out cross-validation (LOOCV) results for internal validation of phase 1 and 2

Comparison	LOOCV mean cutoff (ms)	LOOCV AUC (Logit-based)	Acc (%)	Se (%)	Sp (%)
AC vs AMC	89.58(89.14 – 90.01)	0.805	80.0	65.0	95.0
AMC vs MAC	118.02(117.41–121.97)	0.930	94.3	86.7	100
Phase 2*	187.91(187.84 – 187.93)	0.772	81.5	80.0	83.3

* Phase 2: post-nCRT mucinous degeneration vs. primary mucinous adenocarcinoma

For distinguishing AC from AMC, LOOCV confirmed the robustness of the 89.14-ms cutoff, yielding a mean optimal cutoff of 89.58 ms (range, 89.14–90.01 ms), with a cross-validated AUC of 0.805, accuracy of 80.0%, sensitivity of 65.0%, and specificity of 95.0%. For distinguishing

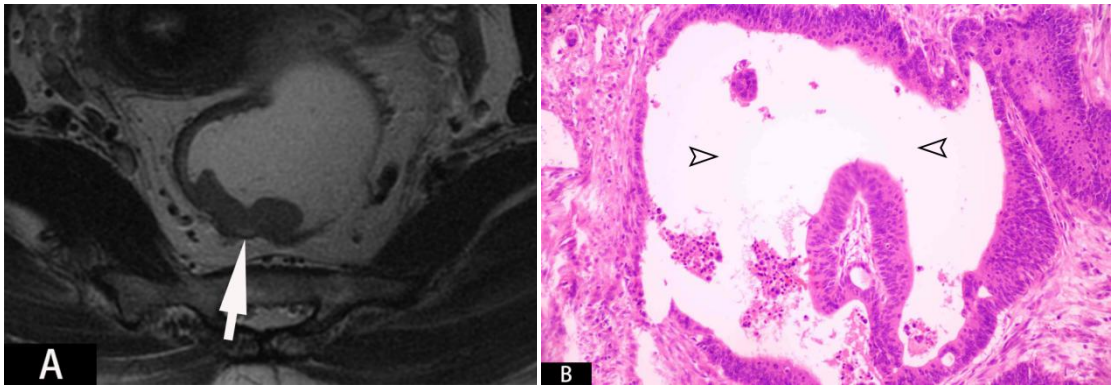
AMC from MAC, LOOCV demonstrated a mean cutoff of 118.02 ms (range, 117.41–121.97 ms) and a cross-validated AUC of 0.930, with accuracy of 94.3%, sensitivity of 86.7%, and specificity of 100%.

For Phase 2 (post-nCRT mucinous degeneration vs. primary mucinous adenocarcinoma), LOOCV revealed a mean optimal cutoff of 187.91 ms (range, 187.84–187.93 ms), with a cross-validated AUC of 0.772, accuracy of 81.5%, sensitivity of 80.0%, and specificity of 83.3%. The extremely narrow cutoff range (0.09 ms) confirms the high stability of the threshold, although the mean value was slightly higher than the original cutoff (181.92 ms), likely attributable to the limited sample size (n=27).

Representative failure cases

To illustrate the potential pitfalls of T2 mapping-based mucin characterization, we present two representative misclassified cases.

Case 1 (false-positive, Phase 1): A patient with pathologically confirmed conventional adenocarcinoma (AC, mucin <5%) was misclassified as AMC based on a T2 value of 89.868 ms, exceeding the 89.14-ms cutoff. Histopathological review confirmed the absence of mucin (Alcian blue negative) but revealed three non-mucinous sources of free water: cystically dilated tumor glands containing serous fluid (primary contributor, open arrows), prominent peritumoral edema with widened interstitial spaces (solid arrows), and dense inflammatory infiltration within the tumor stroma (open long arrows) (Figure 9B–D). These non-mucinous free-water pools elevated the T2 relaxation time, mimicking the signature of mucin and resulting in false-positive classification.



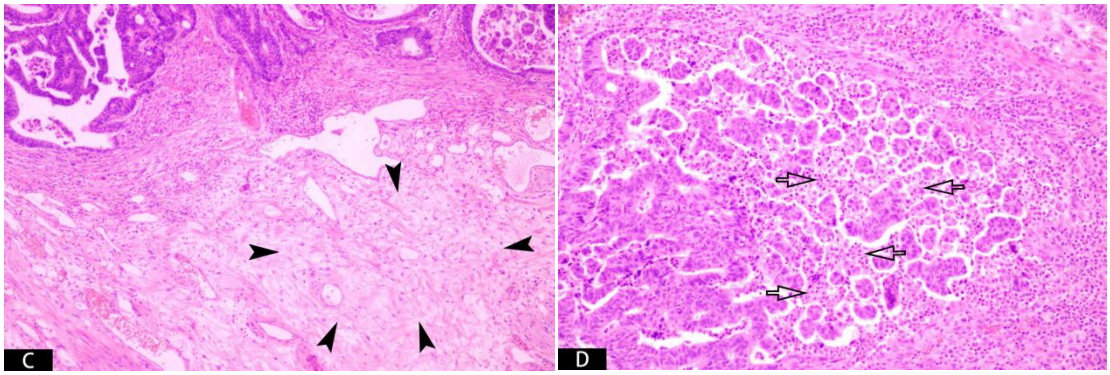
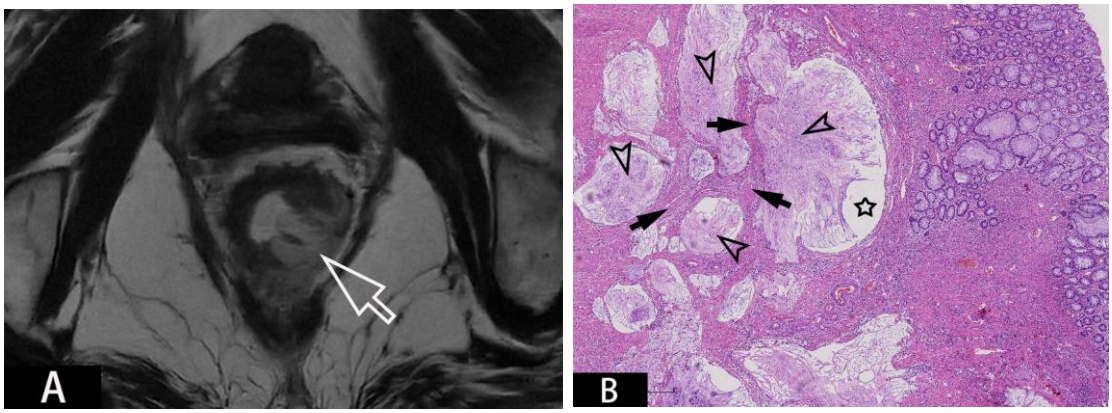


Figure 9. Representative false-positive case: conventional adenocarcinoma (AC) misclassified as AMC due to T2 prolongation. (A) Oblique axial T2-weighted image shows a rectal tumor with a markedly hyperintense cystic area (solid long arrow), corresponding to cystically dilated tumor glands. (B) High-power magnification (HE, ×200) reveals cystically dilated tumor glands (open arrows) containing serous/pale fluid, which serve as the primary source of free water and T2 prolongation. (C) Low-power view (HE, ×100) demonstrates peritumoral edema with widened interstitial spaces (solid arrows), contributing additional free water. (D) High-power view (HE, ×200) shows dense inflammatory infiltration (open long arrows) within the tumor stroma, further increasing tissue free water content. The elevated T2 value in this non-mucinous adenocarcinoma (measured as 89.868 ms, exceeding the AC-vs-AMC cutoff of 89.14 ms) led to misclassification as mucinous adenocarcinoma.

Case 2 (false-positive, Phase 2): A patient with post-nCRT mucinous degeneration was misclassified as primary mucinous adenocarcinoma based on a T2 value of 178.632 ms, below the 181.92-ms cutoff. Histopathology demonstrated that the mucin lakes were not pure acellular pools but rather contained two predominant T2-shortening components: degenerated tumor cell nests floating within the mucin (open arrows) and reticular collagen fibers traversing the mucin lakes (solid long arrows), which partitioned the mucin into small compartments and reduced the proportion of free water (Figure 10B–C). These components—cellular elements (bound water, macromolecular proteins) and collagen (water binding, reduced free water)—shortened the T2 relaxation time, causing the measured T2 value to overlap with that of primary MAC and resulting in false-positive classification.



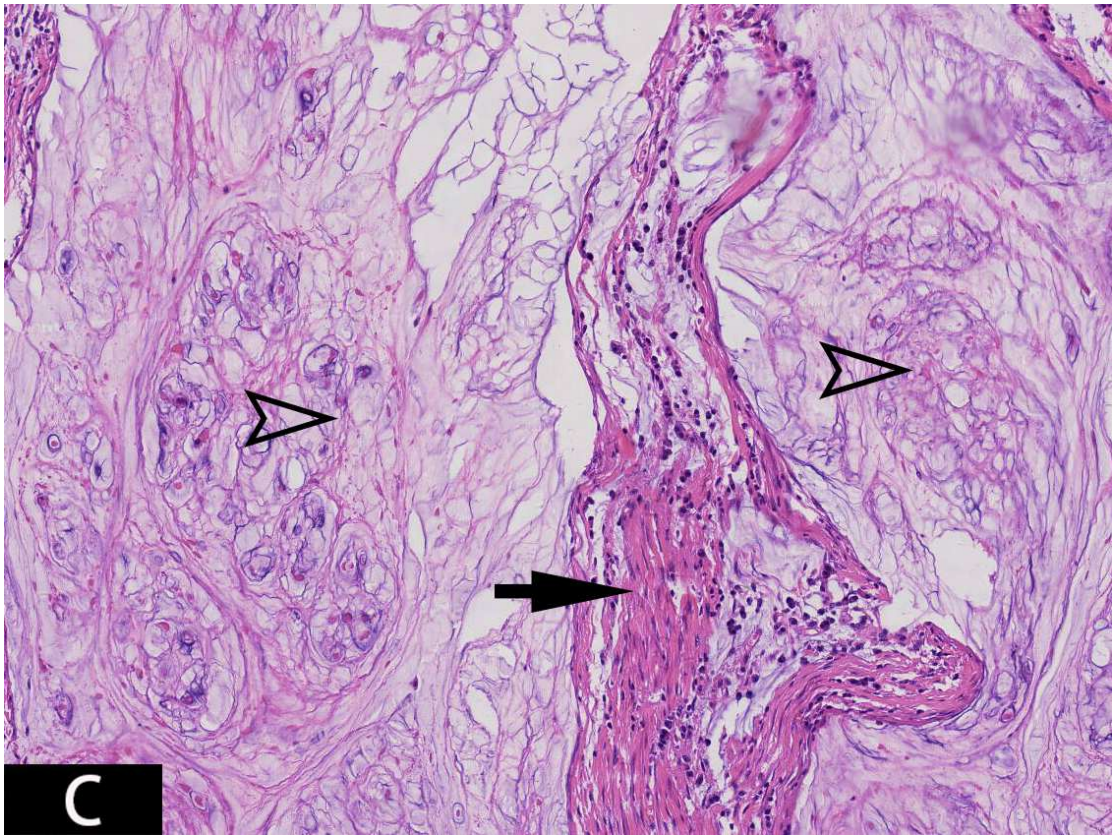


Figure 10. Representative false-positive case: post-nCRT mucinous degeneration misclassified as primary mucinous adenocarcinoma due to T2 shortening. (A) Oblique axial T2-weighted image shows a hyperintense lesion in the tumor bed (open long arrow). (B) Low-power histopathology (HE, ×100) reveals degenerated tumor cell nests (open arrows) floating within the mucin lakes and reticular collagen fibers (solid long arrows) traversing the mucin lakes, partitioning the mucin into small compartments. (C) High-power view (HE, ×200) demonstrates degenerated tumor cell nests (open arrows) floating within the mucin; reticular collagen fibers (solid long arrows) bind water molecules and reduce the proportion of free water. These two factors collectively resulted in a decreased mean T2 value within the mucin lakes, falling into the range of primary mucinous adenocarcinoma and leading to misclassification. T2 mapping yielded a mean T2 value of 178.632 ms, below the 181.92-ms cutoff, resulting in misclassification as primary mucinous adenocarcinoma.

The corresponding T2-weighted images, T2 maps, and histopathological correlates for both cases are shown in Figure 9 (Case 1) and Figure 10 (Case 2).

Discussion

In this study, we asked whether T2 mapping could do two things: first, quantify mucin content across the full spectrum of rectal cancers, and second, solve a real clinical problem—telling apart post-treatment mucinous degeneration from primary mucinous adenocarcinoma. Our findings

suggest that T2 values correlate strongly with pathological mucin content and may effectively discriminate among tumors with varying mucin proportions. Furthermore, T2 mapping appears to show good diagnostic performance in distinguishing post-neoadjuvant mucinous degeneration from primary mucinous adenocarcinoma, potentially addressing a clinically relevant diagnostic challenge that warrants further prospective investigation.

Quantitative Assessment of Mucin Content with T2 Mapping

The strong positive correlation between T2 values and pathological mucin content (Rs = 0.877) establishes T2 mapping as a valid quantitative biomarker for mucin assessment. This finding aligns with the biophysical basis that mucin, composed of hydrophilic glycoproteins, prolongs T2 relaxation times due to increased water content and altered macromolecular environment [[12]]. The progressive increase in T2 values across the three groups (AC: 82.48 ± 5.35 ms; AMC: 92.86 ± 10.14 ms; MAC: 160.73 ± 33.19 ms) reflects the pathological progression from no mucin to focal/small amounts of mucin and then to diffuse/large amounts of mucin. The cutoff values for different comparisons (89.14 ms, 93.72 ms, 117.92 ms) increased sequentially, corresponding to the increasing trend of T2 values among the three groups.

In this study, the T2 value ranges of AC and MAC were completely separated (AC maximum 89.868 ms < MAC minimum 97.566 ms), yielding an AUC of 1.000. The mean T2 value of the AMC group (92.86 ms) was close to the lower limit of this separation interval, while the MAC group mean (160.73 ms) was far above the upper limit. This indicates that the presence of mucin (even focal) significantly elevates T2 values, while extensive mucin lakes cause a further sharp increase. The clinical implication of this complete separation is that preoperative T2 mapping can accurately identify MAC. Since MAC is associated with poor response to nCRT, higher rates of recurrence and metastasis, preoperative identification can guide treatment decisions (e.g., intensifying neoadjuvant regimens, expanding surgical margins, or proceeding directly to surgery). When the two groups are completely separated, the optimal cutoff value is not unique but any value between the AC maximum and MAC minimum (89.868–97.566 ms). The Youden index gave 93.717 ms, which lies within the transitional range of T2 values across the three groups (AC 82.48, AMC 92.86, MAC 160.73). Any threshold within this interval can separate AC (no or minimal mucin) from mucin-containing lesions (both focal and diffuse). In clinical practice, a lower threshold (e.g., 90 ms) may be used for screening sensitivity, whereas a higher threshold (e.g., 97 ms) may be used for diagnostic specificity.

For distinguishing AMC from MAC, the AUC was 0.9867 (95% CI: 0.966–1.000), with an optimal cutoff of 117.92 ms, specificity of 100%, and sensitivity of 93.33%. This cutoff is much higher than the AMC mean (92.86 ms) and lower than the MAC mean (160.73 ms), indicating that it effectively

differentiates focal/small amounts of mucin from diffuse/large amounts of mucin. When T2 exceeds 117.9 ms, pure MAC is highly suspected. This cutoff also performed excellently in distinguishing MAC from non-MAC (including AC and AMC) (AUC 0.9933, specificity 100%), further supporting a dose-response relationship between T2 values and the abundance of mucin lakes. Meanwhile, the World Health Organization defines mucinous adenocarcinoma as ≥50% mucinous component [1]; the optimal cutoff of 117.92 ms provides a quantitative reference for this definition.

For distinguishing AC from AMC, the AUC was 0.8175 (95% CI: 0.691–0.943), with an optimal cutoff of 89.14 ms, sensitivity of 95%, and specificity of 70%. This cutoff is close to the AMC mean (92.86 ms) and slightly higher than the AC mean (82.48 ms), thus capturing the vast majority of AMC (95%) but resulting in a 30% false-positive rate due to some AC cases having T2 values above this threshold (e.g., due to edema, inflammation). When the comparison was expanded to "mucinous lesions (MAC+AMC)" versus AC, the cutoff of 90.013 ms increased specificity to 100% but decreased sensitivity to 80%. This indicates that a slight increase in the threshold can completely exclude AC but will miss about 20% of mucinous lesions, mainly those with small amounts of mucin (whose T2 values fluctuate around the threshold). The strong correlation between T2 values and mucin content (Rs = 0.877) explains this phenomenon of decreased sensitivity with increased threshold, which essentially reflects the continuous distribution of mucin content.

Our leave-one-out cross-validation (LOOCV) further confirmed the robustness of these cutoffs. For AC versus AMC, the LOOCV-derived mean cutoff was 89.58 ms (range, 89.14–90.01 ms), with a cross-validated AUC of 0.805, accuracy of 80.0%, sensitivity of 65.0%, and specificity of 95.0%. For AMC versus MAC, the mean cutoff was 118.02 ms (range, 117.41–121.97 ms), with a cross-validated AUC of 0.930, accuracy of 94.3%, sensitivity of 86.7%, and specificity of 100%. The extremely narrow ranges of the LOOCV cutoffs (within 0.9 ms and 4.6 ms, respectively) confirm that the thresholds are stable and not overfitted to the discovery cohort. The modest reduction in cross-validated sensitivity compared to the original estimates (e.g., 65% vs. 95% for AC vs. AMC) reflects the expected optimism due to limited sample size and the inherent variability of Youden index-based threshold selection, and underscores the need for external validation in larger cohorts.

Our results share similarities but also important differences with the findings of Zhang et al. [12]. Zhang et al. used a T2 cutoff of 80 ms to distinguish mucinous from non-mucinous rectal cancer, with 100% sensitivity and 97% specificity. In comparison, our optimal cutoff for the same population (MAC vs. non-MAC) was notably higher (117.92 ms), yet the diagnostic performance remained excellent (AUC 0.9933 vs. 0.999). The discrepancy in cutoff values may be because our non-MAC group included "adenocarcinoma with mucinous component" (mucin <50%), which have higher T2 values than typical pure adenocarcinomas, thereby raising the threshold needed to

differentiate MAC. Zhang et al. may have strictly excluded such intermediate tumors, resulting in a lower baseline T2 in the non-mucinous group and a consequently smaller cutoff. Building on similar findings to [12], our study included an AMC group (mucin <50%), covering the complete spectrum from pure adenocarcinoma, through adenocarcinoma with a mucinous component, to pure mucinous adenocarcinoma, more closely reflecting real-world clinical practice. We found a stepwise positive correlation between T2 values and mucin content, with pairwise AUCs of 0.8175 and 0.9867, indicating that T2 mapping can not only discriminate MAC from non-MAC but also semi-quantitatively reflect the degree of mucin content, facilitating more refined preoperative assessment.

Our results complement and extend previous studies using diffusion-weighted imaging (DWI) for mucinous tumor characterization. While DWI-derived apparent diffusion coefficient (ADC) values have been used to distinguish mucinous from non-mucinous rectal cancer [12, 22, 23], ADC measurements are influenced by both cellularity and microperfusion, leading to inherent confounding in interpretation. In contrast, T2 mapping directly probes the water content and macromolecular environment within mucin lakes, without interference from cellular or perfusion factors, and can more specifically reflect the biochemical characteristics of mucin, thereby providing quantitative information that is complementary to ADC and more pathologically specific.

Distinguishing Post-nCRT Mucinous Degeneration from Primary Mucinous Adenocarcinoma

In patients with locally advanced rectal cancer receiving neoadjuvant chemoradiotherapy, some originally non-mucinous adenocarcinomas may develop treatment-induced mucinous degeneration, pathologically characterized by acellular mucin lakes with no or only minimal residual tumor cells. This treatment-induced mucinous degeneration usually indicates a favorable response to therapy, relatively good prognosis, and may even make patients eligible for organ-preserving strategies or less extensive surgery [9]. However, the clinical dilemma is to distinguish between treatment-induced mucinous degeneration (benign) and primary or residual mucinous adenocarcinoma (malignant). Both present as hyperintense signals on conventional T2-weighted MRI because mucin itself is rich in bound water, and conventional imaging cannot reliably determine whether viable tumor cells are present within the mucin lakes [10, 11]. This diagnostic difficulty leads to significant clinical consequences: misinterpreting a good responder with mucinous degeneration as having residual MAC may lead to unnecessary radical surgery or extended resection; conversely, misdiagnosing true MAC as benign degeneration may delay curative treatment. Therefore, establishing a non-invasive imaging method that reliably distinguishes these two mucinous entities has important clinical value [24].

Our findings demonstrate that T2 values in post-treatment acellular mucinous degeneration (198.76

ms) were significantly higher than those in primary mucinous adenocarcinoma (156.34 ms), with a statistically significant difference ($P < 0.05$). This difference can be explained histopathologically: acellular mucin lakes consist mainly of free water [25], allowing free water molecule movement and prolonged T2 relaxation times; in contrast, primary mucinous adenocarcinoma, although containing abundant mucin, still harbors viable tumor cells floating within the mucin lakes. The presence of cellular components restricts water molecule motion, and the intracellular macromolecular environment (e.g., proteins) also shortens T2 relaxation times, resulting in relatively lower T2 values.

Diagnostic performance analysis showed that T2 mapping achieved an AUC of 0.825 for distinguishing the two entities, with a sensitivity of 0.83 and specificity of 0.80, and an optimal cutoff of 181.92 ms. This cutoff lies between the mean T2 values of the two groups and can serve as a clinical reference: T2 values above 181.92 ms tend to indicate acellular mucin lakes (favorable response), while values below this threshold raise suspicion for primary mucinous adenocarcinoma. These results support T2 mapping as a quantitative adjunctive tool for differentiating these two lesions, providing objective evidence for individualized decision-making after neoadjuvant therapy.

LOOCV for Phase 2 yielded a mean optimal cutoff of 187.91 ms (range, 187.84–187.93 ms), with a cross-validated AUC of 0.772, accuracy of 81.5%, sensitivity of 80.0%, and specificity of 83.3%. Although the LOOCV mean cutoff was slightly higher than the original cutoff (181.92 ms), the range was extremely narrow (0.09 ms), confirming that the threshold is highly reproducible across different training subsets. The minor upward shift is likely attributable to the limited sample size (n=27) and the inherent variability of Youden index estimation in small cohorts, and does not undermine the clinical utility of the cutoff. Notably, the cross-validated AUC (0.772) was lower than the original AUC (0.825), reflecting the expected performance shrinkage due to small sample size; nevertheless, the value remains above 0.75, indicating clinically meaningful discriminatory ability.

Pitfalls in T2 interpretation: insights from misclassified cases

Having established the discriminative performance of T2 mapping in both phases, we next examined the misclassified cases to understand the underlying biological confounders. Two representative false-positive cases—one from Phase 1 (AC misclassified as AMC) and one from Phase 2 (post-nCRT mucinous degeneration misclassified as primary MAC)—illustrate a fundamental limitation of single-parameter T2 mapping: the measured T2 value reflects the composite signal from all proton pools within a voxel and cannot distinguish free water from bound water, nor differentiate the biological source of water[26].

In the false-positive Phase 1 case (AC misclassified as AMC), histopathology confirmed the absence of mucin but revealed three non-mucinous sources of free water: cystically dilated tumor glands containing serous fluid (primary contributor, open arrows), peritumoral and interstitial edema (solid arrows), and dense inflammatory infiltration (open long arrows). These conditions collectively prolonged T2 relaxation and mimicked the T2 signature of mucin. This case demonstrates that any pathological process that increases tissue free water content—whether mucin, edema, cystic fluid, or inflammation—may confound the diagnosis of mucinous components[27].

Conversely, in the false-positive Phase 2 case (post-nCRT mucinous degeneration misclassified as MAC), the mucin lakes contained two predominant T2-shortening components: degenerated tumor cell nests floating within the mucin (open arrows) and reticular collagen fibers traversing the mucin lakes (solid long arrows), which partitioned the mucin and reduced free water proportion. These components—cellular bound water and collagenous water binding—collectively shortened T2 relaxation, lowering the measured T2 value into the range of primary MAC[28, 29].

Taken together, these two cases illustrate the dual directionality of T2 confounding: T2 can be prolonged by non-mucinous free water, leading to false-positive AMC diagnoses, or shortened by cellular/fibrous infiltration of mucin lakes, leading to false-positive MAC diagnoses. This bidirectional confound cannot be resolved by T2 mapping alone, but may be addressed by integrating morphological features (e.g., T2WI signal heterogeneity, fibrotic strands) with diffusion-weighted imaging, where ADC can differentiate cellular tissues (low ADC) from edema or cystic fluid (high ADC)[30]. Multi-parametric approaches incorporating T2 mapping, DWI, and morphological assessment are likely to improve diagnostic accuracy in challenging cases with overlapping T2 values.

To our knowledge, this is the first study to directly compare T2 values of mucinous components between post-nCRT mucinous degeneration and primary mucinous adenocarcinoma. Through this exploratory study, we provide preliminary evidence that may assist clinicians in differentiating whether post-treatment mucinous changes represent a benign treatment response or primary MAC. Furthermore, we speculate that if a patient with MAC achieves a good pathological response to nCRT – i.e., tumor cell death and conversion of mucin lakes to an acellular state – their T2 values might also decrease from baseline. Of course, this hypothesis requires prospective longitudinal validation, i.e., enrolling patients with confirmed MAC and performing T2 mapping both before and after nCRT. The quantitative cutoffs provided in this study may serve as a reference for the design and sample size estimation of such future investigations but should not be directly applied in clinical practice until externally validated.

Clinical Implications

The results of this study suggest several potential clinical applications that warrant further investigation. First, preoperative quantitative assessment of mucin content using T2 mapping may offer a non-invasive tool to inform treatment planning for primary rectal cancer. MAC is often associated with distinct response patterns to nCRT, and some studies suggest reduced sensitivity [31, 32]. If validated in prospective cohorts, accurate identification of MAC before treatment could potentially aid in decisions regarding neoadjuvant regimen selection or surgical approach. Second, for patients who have undergone nCRT, distinguishing treatment-induced mucinous degeneration from residual MAC may contribute to response assessment. Should these findings be confirmed, patients with extensive mucinous degeneration representing major pathological response might be considered for organ-preserving strategies or less extensive surgery [33]. Conversely, persistent MAC with viable tumor cells would still warrant completion total mesorectal excision and close surveillance according to current standards of care. Third, the quantitative nature of T2 mapping may facilitate standardized reporting and reduce interobserver variability inherent in qualitative image interpretation. The excellent interobserver agreement observed in this study (ICC >0.90) supports the reproducibility of this approach. However, we emphasize that all proposed clinical applications are preliminary and derived from a single-center retrospective cohort; prospective validation is required before any of these thresholds or algorithms can be integrated into routine clinical decision-making.

Limitations

This study has several limitations. First, it is a single-center retrospective study with a relatively small sample size, particularly in Phase 2 (n=27). LOOCV partially mitigated overfitting concerns by demonstrating narrow cutoff ranges; however, cross-validated sensitivity for AC versus AMC decreased from 95% to 65%, and the cross-validated AUC for Phase 2 dropped from 0.825 to 0.772, reflecting expected performance shrinkage due to limited sample size and the inherent variability of Youden index estimation. These findings underscore the need for external validation before clinical translation. Second, histopathological quantification of mucin content was semiquantitative rather than automated, which may have underestimated the strength of correlations. Third, formal radiology-pathology co-registration using fiducial markers was not performed due to the retrospective design. Instead, MRI-pathology matching was performed at the whole-tumor or regional level using anatomical landmarks, which may have introduced partial volume effects and imprecision in T2-mucin correlation. Fourth, all cutoffs were derived from a single institutional cohort and have not been tested in an independent external cohort. The generalizability of the proposed T2 thresholds (89.14 ms, 117.92 ms, and 181.92 ms) to other populations, scanners, or protocols remains to be established. Multicenter prospective studies with standardized protocols are warranted to confirm our findings and refine cutoffs for broader application.

Conclusion

T2 mapping enables quantitative assessment of mucin content in rectal cancer, demonstrating a strong positive correlation with pathological mucin content and effective discrimination among tumors with varying mucin proportions. Furthermore, T2 mapping distinguishes post-nCRT mucinous degeneration from primary mucinous adenocarcinoma with good diagnostic performance. These findings support T2 mapping as a valuable quantitative imaging tool for preoperative characterization of mucinous components in rectal cancer, with potential implications for treatment planning and response assessment.

Reference

1. Luo C, Cen S, Ding G, Wu W. Mucinous colorectal adenocarcinoma: clinical pathology and treatment options. *Cancer communications (London, England)* 2019; 39:13
2. Zhu L, Ling C, Xu T, et al. Clinicopathological Features and Survival of Signet-Ring Cell Carcinoma and Mucinous Adenocarcinoma of Right Colon, Left Colon, and Rectum. *Pathology oncology research : POR* 2021; 27:1609800
3. Song W, Wu SJ, He YL, et al. Clinicopathologic features and survival of patients with colorectal mucinous, signet-ring cell or non-mucinous adenocarcinoma: experience at an institution in southern China. *Chinese medical journal* 2009; 122:1486-1491
4. Huang A, Yang Y, Shi JY, et al. Mucinous adenocarcinoma: A unique clinicopathological subtype in colorectal cancer. *World journal of gastrointestinal surgery* 2021; 13:1567-1583
5. Zhang J, Xie X, Wu Z, et al. Mucinous Adenocarcinoma Predicts Poor Response and Prognosis in Patients With Locally Advanced Rectal Cancer: A Pooled Analysis of Individual Participant Data From 3 Prospective Studies. *Clinical colorectal cancer* 2021; 20:e240-e248
6. Chou CL, Chen TJ, Tian YF, et al. Upregulated MUC2 Is an Unfavorable Prognostic Indicator for Rectal Cancer Patients Undergoing Preoperative CCRT. *Journal of clinical medicine* 2021; 10
7. Elomaa H, Tarkiainen V, Äijälä VK, et al. Associations of mucinous differentiation and mucin expression with immune cell infiltration and prognosis in colorectal adenocarcinoma. *British journal of cancer* 2025; 132:660-669
8. Kalisz KR, Enzerra MD, Paspulati RM. MRI Evaluation of the Response of Rectal Cancer to Neoadjuvant Chemoradiation Therapy. *Radiographics : a review publication of the Radiological Society of North America, Inc* 2019; 39:538-556
9. Miranda J, Pinto PVA, Kinochita F, et al. Mucinous Degeneration on MRI After Neoadjuvant Therapy in Patients With Rectal Adenocarcinoma: Frequency and Association With Clinical Outcomes. *AJR American journal of roentgenology* 2023; 221:206-216
10. Corines MJ, Ibrahim A, Baheti A, et al. Can MRI radiomics distinguish residual adenocarcinoma from acellular mucin in treated rectal cancer? *European journal of radiology*

2025; 184:111986

11. Judge SJ, Malekzadeh P, Corines MJ, et al. Watch and wait in rectal cancer patients with residual mucin on magnetic resonance imaging following neoadjuvant therapy. *Journal of the National Cancer Institute* 2024; 116:1761-1766
12. Zhang J, Ge Y, Zhang H, Wang Z, Dou W, Hu S. Quantitative T2 Mapping to Discriminate Mucinous from Nonmucinous Adenocarcinoma in Rectal Cancer: Comparison with Diffusion-weighted Imaging. *Magnetic resonance in medical sciences : MRMS : an official journal of Japan Society of Magnetic Resonance in Medicine* 2022; 21:593-598
13. Yan C, Yang H, Chen L, et al. Clinical significance of mucinous component in colorectal adenocarcinoma: a propensity score-matched study. *BMC cancer* 2021; 21:1286
14. Patel UB, Taylor F, Blomqvist L, et al. Magnetic resonance imaging-detected tumor response for locally advanced rectal cancer predicts survival outcomes: MERCURY experience. *Journal of clinical oncology : official journal of the American Society of Clinical Oncology* 2011; 29:3753-3760
15. Zager Y, Horesh N, Abdelmasseh M, et al. The predicting value of post neoadjuvant treatment magnetic resonance imaging: a meta-analysis. *Surgical endoscopy* 2024; 38:6846-6853
16. Sheedy SP, Arya S, Baheti AD, et al. SAR Disease-focused Panel: Restaging Rectal Cancer MRI Synoptic Report-User Guide with Imaging Review. *Radiographics : a review publication of the Radiological Society of North America, Inc* 2025; 45:e250006
17. Dresen E. Challenges in Restaging of Rectal Cancer. *Journal of the Belgian Society of Radiology* 2025; 109
18. Shia J, Guillem JG, Moore HG, et al. Patterns of morphologic alteration in residual rectal carcinoma following preoperative chemoradiation and their association with long-term outcome. *The American journal of surgical pathology* 2004; 28:215-223
19. Wang F, Chen G, Zhang Z, et al. The Chinese Society of Clinical Oncology (CSCO): Clinical guidelines for the diagnosis and treatment of colorectal cancer, 2024 update. *Cancer communications (London, England)* 2025; 45:332-379
20. Nagtegaal ID, Odze RD, Klimstra D, et al. The 2019 WHO classification of tumours of the digestive system. *Histopathology* 2020; 76:182-188
21. Jäger T, Neureiter D, Urbas R, et al. Applicability of American Joint Committee on Cancer and College of American Pathologists Regression Grading System in Rectal Cancer. *Diseases of the colon and rectum* 2017; 60:815-826
22. Cao W, Li B, Gong J, et al. Diffusion-weighted magnetic resonance imaging of mucin pools in locally advanced rectal mucinous adenocarcinoma predicts tumor response to neoadjuvant therapy. *European journal of radiology* 2020; 125:108890
23. El Homsi M, Mazaheri Y, Kuten J, et al. Can ADC differentiate cellular from acellular mucin in mucinous adenocarcinoma tumor beds after treatment of rectal cancer? A multicenter study. *European radiology* 2026;
24. Kim DJ, Kim JH, Lim JS, et al. Restaging of Rectal Cancer with MR Imaging after Concurrent Chemotherapy and Radiation Therapy. *Radiographics : a review publication of the Radiological*

Society of North America, Inc 2010; 30:503-516

25. Dworak O, Keilholz L, Hoffmann A. Pathological features of rectal cancer after preoperative radiochemotherapy. *International journal of colorectal disease* 1997; 12:19-23
26. Bottomley PA, Foster TH, Argersinger RE, Pfeifer LM. A review of normal tissue hydrogen NMR relaxation times and relaxation mechanisms from 1-100 MHz: dependence on tissue type, NMR frequency, temperature, species, excision, and age. *Medical physics* 1984; 11:425-448
27. O'Brien AT, Gil KE, Varghese J, Simonetti OP, Zareba KM. T2 mapping in myocardial disease: a comprehensive review. *Journal of cardiovascular magnetic resonance : official journal of the Society for Cardiovascular Magnetic Resonance* 2022; 24:33
28. Bradley WG, Jr. MR appearance of hemorrhage in the brain. *Radiology* 1993; 189:15-26
29. Xue S, Zhu Y, Shao M, et al. T1/T2 mapping as a non-invasive method for evaluating liver fibrosis based on correlation of biomarkers: a preclinical study. *BMC gastroenterology* 2025; 25:122
30. Koh DM, Collins DJ. Diffusion-weighted MRI in the body: applications and challenges in oncology. *AJR American journal of roentgenology* 2007; 188:1622-1635
31. McCawley N, Clancy C, O'Neill BD, Deasy J, McNamara DA, Burke JP. Mucinous Rectal Adenocarcinoma Is Associated with a Poor Response to Neoadjuvant Chemoradiotherapy: A Systematic Review and Meta-analysis. *Diseases of the colon and rectum* 2016; 59:1200-1208
32. Tan X, Zhang Y, Wu X, et al. Mucinous histology is a negative predictor of neoadjuvant chemoradiotherapy for locally advanced rectal adenocarcinoma. *BMC gastroenterology* 2024; 24:263
33. Ouyang K, Yang Z, Yang Y, Lyu Z, Wang J, Li Y. Effectiveness of Organ Preservation for Locally Advanced Rectal Cancer With Complete Clinical Response After Neoadjuvant Chemoradiotherapy: Bayesian Network Meta-analysis. *Diseases of the colon and rectum* 2025; 68:287-298